

See discussions, stats, and author profiles for this publication at: <https://www.researchgate.net/publication/231370931>

Prediction of the Salting-Out Effect of Strong Electrolytes on Water + Alkane Solutions

ARTICLE *in* INDUSTRIAL & ENGINEERING CHEMISTRY RESEARCH · JULY 2003

Impact Factor: 2.59 · DOI: 10.1021/ie020918u

CITATIONS

69

READS

37

4 AUTHORS, INCLUDING:



Patrice Paricaud

ENSTA-ParisTech, Université Paris-Saclay

42 PUBLICATIONS **802** CITATIONS

SEE PROFILE



Amparo Galindo

Imperial College London

117 PUBLICATIONS **3,824** CITATIONS

SEE PROFILE



Geoffrey C Maitland

Imperial College London

130 PUBLICATIONS **2,953** CITATIONS

SEE PROFILE

Prediction of the Salting-Out Effect of Strong Electrolytes on Water + Alkane Solutions

B. H. Patel,[†] P. Paricaud,[†] A. Galindo,^{*,†} and G. C. Maitland[‡]

Department of Chemical Engineering and Chemical Technology, Imperial College London, South Kensington Campus, London SW7 2AZ, United Kingdom, and Schlumberger Cambridge Research, High Cross, Maddingley Road, Cambridge CB3 0EL, United Kingdom

In this work we investigate the salting out of *n*-alkanes in water by strong electrolytes using an extension of the statistical associating fluid theory for attractive potentials of variable range which incorporates ionic interactions (SAFT-VRE) [Galindo, A.; Gil-Villegas, A.; Jackson, G.; Burgess, A. N. *J. Phys. Chem. B* **1999**, 103, 10272]. The systems are treated as water (1) + *n*-alkane (2) + cation (3) + anion (4) four-component mixtures. The water molecules are modeled as spherical with four associating sites to mediate hydrogen bonding, while the *n*-alkane molecules are modeled as chains of tangentially bonded spherical segments interacting via square-well potentials. The phase behavior of the binary water + *n*-alkane mixtures is well-described by the theoretical approach using two unlike adjustable parameters which are transferable for different alkane molecules. The salt is incorporated in the model as fully dissociated and assumed to be present only in the water-rich phase. In this way, the anion and cation are modeled as two hard spheres of different diameters in what concerns their repulsive contribution. The experimental Pauling radii are used for each of the ions. Long-range Coulombic ion–ion interactions are treated in the mean spherical approximation at the level of the restricted primitive model, and the experimental water dielectric constant *D* is incorporated to model ion–solvent electrostatic interactions. Water–ion attractive interactions are treated following previous work for aqueous solutions. We find that, to observe the desired salting-out effect in the mixture, no additional adjustable parameters are required. In this sense, the theoretical calculations are true predictions of the phase behavior of these complex mixtures.

1. Introduction

Dissolved salts dramatically affect the phase equilibria of aqueous solutions. This can become an advantage in processes such as salting out, where the drying of an organic solvent from an aqueous solution is carried out by adding salt. Depending on the nature of the ionic and organic components, however, both salting out (drying) and salting in (wetting) are observed.¹ In the context of many chemical and geological processes it is also important to determine the precise effect of dissolved salts on the phase behavior of mixed solvent systems. In this work we study the solubility of hydrocarbon molecules (*n*-alkanes) in water and the changes that take place in this phase behavior by the addition of alkali halide salts (XY, X = Li⁺, Na⁺, K⁺, and Y = Cl[−], Br[−], I[−]). We use an equation of state which combines the SAFT framework with added contributions to take into account the ion–ion and solvent–ion interactions. The strength of our approach is that it can be used for nonelectrolyte as well as for electrolyte systems in wide ranges of pressure and temperature.

Electrolyte solutions pose a considerable theoretical challenge due to the long-range nature of charge–charge Coulombic interactions, and to the fact that many common solvents are highly polar and, as in the case of water, may present strong hydrogen-bonding

interactions. In the seminal work of Debye and Hückel^{2,3} the statistical mechanics of a solution of point charges is solved by treating the solvent at the level of a dielectric continuum (so-called McMillan–Mayer or primitive model). This model is exact in the limit of infinite dilution, but it finds very limited applicability for comparison with experimental data at intermediate concentration ranges. Integral equation approaches such as the mean spherical approximation (MSA)⁴ have more recently been used to study electrolyte solutions incorporating both charge sizes and the solvent explicitly (Lewis–Randall or nonprimitive models). In particular, the MSA has been solved for mixtures of ionic and dipolar species.^{5,6} It seems clear that, as well as incorporating the ionic effects, solvent–solvent and solvent–ion interactions need to be incorporated in some detail to obtain an accurate description of the phase behavior of aqueous electrolyte solutions in wide ranges of salt concentration. Furthermore, to consider salting-out effects, mixed solvent systems are of special interest. It is not possible, however, to consider mixed solvent systems within a McMillan–Mayer model. Lee and co-workers^{7–9} have studied a number of mixed solvent systems using a molecular approach that involves the Gibbs–Duhem relation and the affinity relation between solvents and solutes, proposing a method to generalize the McMillan–Mayer model to mixed solvent solutions. On the other hand, a number of engineering approaches have been developed which combine both frameworks. Activity coefficient methods such as UNIQUAC and the NRTL¹⁰ equation have been combined with extended forms of the Debye–Hückel theory and have been used

* To whom correspondence should be addressed. Tel.: 44 (0)20 75945606. Fax: 44 (0)20 75945604. E-mail: a.galindo@imperial.ac.uk.

[†] Imperial College London.

[‡] Schlumberger Cambridge Research.

to model single and mixed solvent electrolyte solutions with some success. Cardoso and O'Connell¹¹ have provided a rigorous derivation of the activity coefficients in models combining the McMillan–Mayer and Lewis–Randall frameworks. A number of studies have involved mixed solvent systems using these activity coefficient models. Chen and co-workers^{12–14} have extended the NRTL approximation to model electrolytes by adding the Pitzer–Debye–Hückel equation¹⁵ to account for the long-range interactions, Zerres and Prausnitz¹⁶ and Kolker and de Pablo^{17–19} later followed a similar technique, and the UNIQUAC approach was used by Sander and Fredenslund²⁰ in combination with a Debye–Hückel term to examine a number of mixed solvent systems. Activity coefficient approaches can provide successful correlations of the experimental data; unfortunately, it is difficult to use them as predictive tools. In particular, these models are limited by the need to select standard states, which means that they are not useful in supercritical conditions.

A more general framework can be obtained from the development of perturbation theories. These approaches are based on expansions of the Helmholtz free energy, from which, by differentiation, other thermodynamic properties can be obtained. Stell and Lebowitz²¹ developed a perturbation expansion for the primitive model, and Henderson et al.²² solved the expansion for an ion–dipole mixture. Very interesting are the works of Chan,^{23,24} who combined the Carnahan–Starling hard-sphere equation with the Debye–Hückel equation and compared it with the results of the expansion of Stell and Lebowitz. Chan was able to observe that the main improvement over the Debye–Hückel model comes from the treatment of the hard-sphere contribution. This idea had, in fact, been used previously by a number of authors, who have combined equations of state in the form of the Helmholtz free energy with electrostatic contributions, using both the Debye–Hückel and the MSA approximations. Raatschen et al.²⁵ combined an equation of state for Lennard–Jones molecules with electrostatic contributions due to the charging of the ions and to the ion–ion interactions. Harvey and Prausnitz²⁶ have examined the phase equilibrium of a water + methane solution at high temperature and pressure in the presence of NaCl, combining the ionic effects with a conventional equation of state. They use the Lennard–Jones intermolecular potential to model all the species in the fluid (including the ionic species) and use a Barker and Henderson perturbation expansion to calculate the free energy. Ion-charging and charge–charge contributions are also taken into account. To obtain quantitative agreement with experimental data, however, they incorporate an ion–methane interaction parameter in addition to the water–salt and water–methane parameters. As we will see later, the approach proposed in our work does not require methane–salt adjustable parameters, meaning that we provide a truly predictive description of the salting-out effect. Wu and Prausnitz²⁷ have extended the Peng–Robinson equation of state to take into account electrostatic and hydrogen-bonding interactions and re-examine the salting-out effects in aqueous solutions of hydrocarbons. These works are specially relevant to our present study. In a similar spirit, Myers et al.²⁸ have combined the Peng–Robinson equation with an ionic contribution and examine the activity coefficients of a large number of electrolyte solutions. It is also important to mention the

works of Jin and Donohue^{29–31} and Economou et al.,³² who have extended the ideas of the perturbed anisotropic chain theory (PACT) to study a large number of aqueous electrolyte systems, although the approach has not been used in mixed solvent solutions, and of Fürst and co-workers,^{33–36} who have performed extensive calculations of the activity coefficients and vapor pressures in single and mixed solvent systems.

We have previously carried out an extension of the statistical associating fluid theory (SAFT) to model electrolyte solutions.^{37,38} The SAFT equation of state is a versatile tool to study the phase behavior of complex fluid mixtures (see ref 39 for a review). It has recently been shown to be also accurate in the description of solid phases of chain fluids^{40,41} and has been extended to study the vapor–liquid interface of associating fluids.⁴² On the basis of the thermodynamic perturbation theory of Wertheim, it is specially suited to modeling of hydrogen-bonding compounds (such as water) and chain molecules (such as *n*-alkanes). Of the many versions of the approach, we have extended the so-called SAFT variable range (SAFT-VR) approach^{37,38,43,44} to study the phase equilibria of a number of aqueous solutions of strong electrolytes in temperature ranges from 0 to 100 °C by adding an extra contribution to the free energy to take into account ion–ion interactions. The solvent is introduced explicitly in the approach with respect to repulsive, dispersive, and hydrogen-bonding interactions, and the solution of the mean-spherical approximation in the restricted primitive model is used to take into account the ionic interactions. The resulting equation turns out to be useful in a predictive sense, requiring one adjustable parameter per ion only, regardless of the salt it forms part of. In this way a table was constructed for three cations (Li^+ , Na^+ , K^+) and three anions (Cl^- , Br^- , I^-), which allows the prediction of the vapor pressure depletion in single-salt³⁷ and mixed-salt systems,^{38,45} in excellent agreement with the experimental data available. Together with this, the increase in density seen for increasing amounts of salt in the solution is also predicted by the approach. The SAFT approach has also been extended by Li and co-workers^{46–48} to study the mean activity coefficients of a large number of 1:1 and 1:2 strong electrolytes including mixed-salt systems,⁴⁶ aqueous solutions of ionic surfactants,⁴⁷ providing also an empirical route for estimating the surface tension and interfacial tension in the surfactant solutions.⁴⁸ In this work we concentrate on the effects of adding salts to solutions of hydrocarbons in water.

A large number of experimental studies are involved with the vapor–liquid equilibria of water + alcohol solutions in the presence of salts as these are useful in the context of extractive distillation. Studies of the salting-out effects in partially miscible liquids are, however, more scarce. Recently, the phase behavior of water + *n*-propanol and water + 2-propanol with added sodium chloride (NaCl), sodium bromide (NaBr), and sodium iodide (NaI) have been measured by Chou et al.⁴⁹ In all cases the addition of salt promotes the phase separation of a water-rich and an alcohol-rich phase (i.e., salting out), with the salt being preferentially found in the water-rich phase. The presence of salt also plays an important role in modifying the liquid–liquid phase equilibria of water–surfactant mixtures. In particular, in the case of mixtures of water + nonionic polyoxyethylene surfactants both a decrease (salting out) and an

increase (salting in) of the lower critical solution temperature has been observed for different added salts. Kenkare et al.¹ used a model mixture of attractive Yukawa spheres and charged spheres to model the micellar (water + surfactant) solution with added salt, solving the Ornstein–Zernike equation with the mean-spherical closure to obtain the thermodynamic properties of the mixture. They were able to reproduce the salting-out effect exhibited when NaCl, NaBr, and NaF were added. The theory, however, was not able to reproduce the salting in seen experimentally when NaI is used. They concluded that excluded volume effects alone cannot account for the difference between salting-out and salting-in effects.

Salting out can also be observed in aqueous solutions of hydrocarbons. Alkane solubility in water is of concern in environmental control, where it is important to predict reliably the hydrocarbon content in the water phase at the level of parts per million. These systems are characterized by a marked immiscibility of the liquid phases, with liquid–liquid separation persisting up to temperatures close and above the critical point of water (647 K). The separation into a hydrocarbon-rich and a water-rich phase is extreme, as indicated by the compositions of the two coexisting phases. It is interesting to note that the solubility of water in the hydrocarbon phase is orders of magnitude greater than the solubility of the oil in water. As expected, the solubility of water decreases monotonically with decreasing temperatures; however, an increase of the oil solubility in water is seen at low temperatures; this unexpected phase behavior remains unexplained. A number of recent works^{50–52} have presented extensive studies of the mutual solubilities of hydrocarbons and water at low temperatures with special emphasis in reproducing the anomalous low-temperature solubility increase. Although the marked immiscibility of these systems means that experimental measurements are difficult, the salting out of methane by NaCl at high pressure has been obtained experimentally.^{53,54} We aim at predicting the salting out of methane by NaCl at high temperatures and pressures, using the data in refs 53 and 54 for comparison with our calculations. As will be shown later, we find that our proposed approach can be used in a truly predictive sense, and hence we also investigate the salting-out effects due to other strong electrolytes. Together with this, we examine closely the mutual solubilities of *n*-alkanes in water, concentrating first in reproducing the unusual increase in oil solubility seen at low temperatures. Salting out by strong electrolytes is later considered. We have placed some emphasis in providing transferable parameters where possible so that a predictive scheme for these complex mixtures can be designed. This paper is organized as follows: in section 2 the molecular models for the pure components and the mixtures are presented, in section 3 the theoretical framework is outlined, and in sections 4 and 5 results and conclusions are given.

2. Molecular Models

In this work we consider only strong electrolytes so that the added salts are assumed to be fully dissociated. In this way, we model the water + oil + salt solutions as four-component systems: water (component 1) + *n*-alkane (2) + cation (3) + anion (4).

2.1. Pure Components. As in previous works, we model the water molecules as hard spheres of diameter

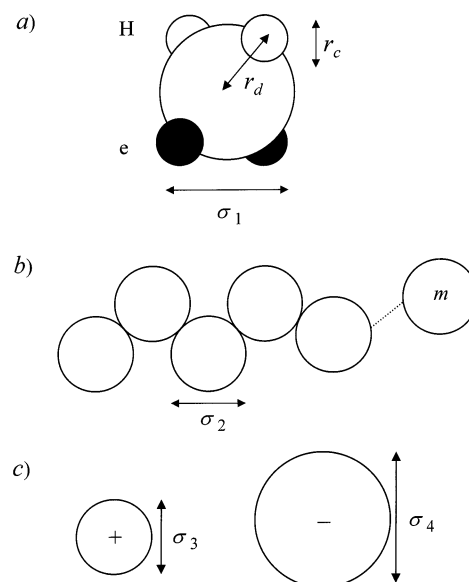


Figure 1. Models for (a) water, (b) *n*-alkanes, and (c) ions. The water molecules are modeled as hard spheres of diameter σ_{11} with four off-center square-well bonding sites. The sites are at a distance r_d from the center of the sphere and have a range r_c . The e and H sites interact with a hydrogen-bonding energy ϵ_{HB} when the site–site distance is within the cutoff distance r_c . (b) The *n*-alkane molecules are modeled as chains of m tangent hard spheres of diameter σ_{22} . (c) The cation and anion are modeled with two hard spheres of diameter σ_{33} and σ_{44} , respectively. Ion–ion interactions are modeled with the mean spherical approximation using an average diameter and the experimental dielectric constant of the solvent. Attractive dispersion interactions are incorporated via a second-order high-temperature perturbation expansion for square-well potentials of range λ_{ij} and depth ϵ_{ij} .

σ_{11} , with four embedded short-ranged attractive sites which mediate the hydrogen bond interactions (see Figure 1); two of the sites are of type H and two of type e, and only H–e bonding is permitted. This model, first proposed by Nezbeda and co-workers,^{55,56} has been used in numerous studies of aqueous solutions.^{57–60} Four associating sites allow the formation of three-dimensional clusters of hydrogen-bonded molecules, which are seen experimentally in water. Although three-site models for water have also been proposed,^{27,61,62} the four-site model is usually preferred following the distributed-charge simulation models for water. The associating sites are placed at a distance $r_d^* = r_d/\sigma_{11}$ from the center of the molecule and have a cutoff range of $r_c^* = r_c/\sigma_{11}$. An attractive square-well interaction of depth $\epsilon_{11}^{\text{HB}}$ occurs when two sites are within r_c^* of each other. Together with this, long-range dispersion interactions are modeled with a square-well potential of range λ_{11} and depth ϵ_{11} . It is important to note at this stage that the dipolar nature of water is not treated explicitly in the model; instead, it is incorporated in an effective way via square-well interactions of variable range and through the association sites which mediate the hydrogen bonding. In addition to this, the dielectric constant of water is taken into account to model the ion–ion screened interactions.

The *n*-alkane molecules are modeled as m_2 tangentially bonded spherical square-well segments of hard-core diameter σ_{22} , range λ_{22} , and depth ϵ_{22} . The parameter m_2 characterizes the chainlike nature of the molecules. A relationship $m_2 = (C - 1)/3 + 1$ has been used to model *n*-alkane molecules in previous works^{43,57,63,64} and has been shown to be valid to model

the phase behavior of polyethylene–solvent systems.⁶⁵ The *n*-alkane molecules are nonpolar and present no hydrogen-bonding interactions; hence, no association sites are incorporated in the model.

In terms of the ionic species, in this work we consider only strong electrolytes, meaning that only fully dissociated cations and anions are taken into account. The cations are modeled as hard spheres of diameter σ_{33} and the anions as hard spheres of diameter σ_{44} . No association sites or square-well dispersion interactions are treated in what concerns ion–ion interactions (either of the same or of opposite charge); only Coulombic interactions are treated. In this respect, the charges are assumed to be immersed in a medium characterized by a dielectric constant D .

It may seem at this stage that the description of the pure component models involves a rather large number of intermolecular parameters. This is due to both the detailed nature of our water model and to the multi-component nature of the system. We have discussed in previous works^{37,38} the importance of incorporating an accurate model for water to study, and to be able to predict, the phase behavior of electrolyte solutions. The pure component parameters for water and the *n*-alkanes are determined from experimental vapor pressure and saturated liquid density data from the triple point to the critical point. In particular, in what relates to our present work, both water and the *n*-alkanes have been used before in the context of the SAFT-VR approach; here, we use the parameters which have been presented elsewhere.^{37,43} In the case of the intermolecular parameters for the ionic components, it is not possible to use vapor pressure data; instead, following previous work,³⁷ we use experimental Pauling diameters⁴ to give values for the hard-sphere diameters of the cation and anion.

2.2. Model Mixtures. To be able to study the phase behavior of the four-component mixture, a large number of unlike mixture parameters would need to be determined. Combining rules, such as the geometric or arithmetic mean of the pure component parameters, are typically used to obtain the mixture parameters. Unfortunately, these rarely provide a good description of complex mixture phase behavior and adjustable parameters need to be introduced. These are usually determined by comparison with experimental data; in this way, the predictive value of most theoretical models is somewhat limited. Our aim in this work is to study the effect of added salts on the phase behavior of water + *n*-alkane mixtures, with a view to provide a truly predictive description of the systems. With this in mind, we have made a number of approximations to reduce the number of cross interactions that need to be considered.

Let us consider first the binary water + *n*-alkane systems. The phase behavior of water + *n*-alkane binary mixtures is characterized by a marked liquid–liquid phase separation, both in composition and in temperature. For example, in the case of a water + *n*-decane mixture, a water-rich phase (containing an oil mole fraction of the order of 10^{-6}) and an oil-rich phase (containing a water mole fraction of the order of 10^{-2}) are seen in coexistence for temperatures up to 500 K. Heavier (larger) alkanes tend to be more immiscible, but even a mixture of water + methane exhibits two immiscible liquid phases for temperatures up to 600 K with water-rich phases of composition 99% water. In our model two unlike adjustable parameters are involved

in the description of water–oil interactions: the range λ_{12} and depth ϵ_{12} of the attractive square well, which characterizes the water–*n*-alkane dispersion interactions. In the SAFT-VR approach, for nonionic compounds the unlike interaction parameters are determined using

$$\epsilon_{12} = (1 - k_{12})\sqrt{(\epsilon_{11}\epsilon_{22})} \quad (1)$$

and

$$\lambda_{12} = (1 - \gamma_{12}) \frac{\lambda_{11}\sigma_{11} + \lambda_{22}\sigma_{22}}{\sigma_{11} + \sigma_{22}} \quad (2)$$

where the adjustable parameters k_{12} and γ_{12} have been determined in order to give the best description of the coexistence of water and oil compositions. Note that the unlike hard-sphere diameter σ_{12} is given exactly as $\sigma_{12} = (\sigma_{11} + \sigma_{22})/2$ and it is not re-adjusted. We used a single set of parameters k_{12} and γ_{12} , which is used in a transferable way to model a series of water + *n*-alkane mixtures, and have placed special emphasis in reproducing the anomalous oil-in-water solubilities. Unfortunately, in the case of the water + methane mixture a different set of parameters needs to be used; it is well-known that methane does not exhibit a phase behavior as corresponding to the first member of the homologous series of the *n*-alkanes (see also ref 57).

In terms of the water + ion interactions, we have already presented in a different work³⁷ a set of unlike parameters that provides an excellent description of the vapor pressure and the density of the solutions for concentrations up to 10 *m*. Water–ion interactions are treated in an effective way via a dielectric constant D and via attractive square wells, which are used to mimic the result of the hydration attractive interactions. The square well is described by two unlike parameters (a range λ_{13} and depth ϵ_{13} are used in the case of water + cation interactions and a range λ_{14} and depth ϵ_{14} in the case of water + anion interactions). The parameters are ion-dependent, rather than salt-dependent, so the phase behavior of mixed-salt systems can be predicted with this approach.^{37,38,45} It should be noted that since our model for pure water does not include dipolar interactions, the dielectric constant of the solution needs to be determined rather arbitrarily. One option is to use it as an adjustable parameter; here, we use instead the experimental value of the dielectric constant^{66,67} of water at each temperature to keep the number of adjustable parameters to a minimum.

To study the phase behavior of water + oil + salt mixtures, it is useful to notice that the extreme phase separation seen in the water + *n*-alkane mixtures means that the water-rich phase can be treated as pure water in relation to the ion–water interactions. Hence, the dielectric constant of pure water at a given temperature is used in each case as in previous work. We consider temperatures from 273 to 623 K and use the experimental data^{66,67} to obtain a correlation,

$$D = -8.6819 \times 10^{-7} T^3 + 1.5363 \times 10^{-3} T^2 - 1.0395 T + 274.70 \quad (3)$$

where the temperature T is in K. The decrease in the dielectric constant with temperature can be clearly seen in Figure 2. The water–ion square-well interactions are modeled using the parameters that were determined in

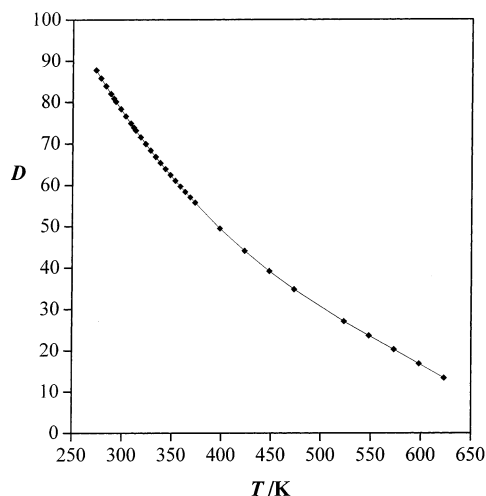


Figure 2. Experimental dielectric constant of water in the saturated liquid phase⁶⁶ compared with correlated values (cf. eq 1). A temperature range from 273 K (melting point) to 647 K (critical point) is presented.

our previous study³⁷ (see also Table 2, and note the typographical error in the ϵ_{ij} values of Table 1 in ref 37), while no ion–oil attractive dispersion interactions are incorporated. The low dielectric constant of the nonpolar *n*-alkane component means that little salt is expected to be present in the oil-rich phase;⁴⁹ in fact, in this work we limit the salt to be present only in the water-rich liquid phase. In the case where vapor phases are also present, these are assumed to be salt-free given the low volatility of the inorganic salts considered in this study.

In this way we will examine the salting-out effects in water + oil mixtures without the need to fit ionic parameters to the four-component mixture; that is, only information on the water + ion and water + oil interactions is needed to predict the expected salting-out effect, as will be shown. Before we consider the result of our calculations, it would be useful to examine some of the theoretical expressions and the conditions for equilibria in the model system proposed.

3. SAFT-VR Equation of State for Electrolytes

We use an extension of the SAFT-VR approach, which incorporates ionic interactions, to describe the thermodynamic properties of the mixtures. The general expressions of the theory have already been presented in detail elsewhere;^{37,38,43,44} here, we concentrate on the expressions for a four-component mixture of water (component 1) + *n*-alkane (component 2) + cation (component 3) + anion (component 4). The free energy can be written in terms of separate contributions as

$$\frac{A}{NkT} = \frac{A^{\text{IDEAL}}}{NkT} + \frac{A^{\text{MONO.}}}{NkT} + \frac{A^{\text{ASSOC.}}}{NkT} + \frac{A^{\text{CHAIN}}}{NkT} + \frac{A^{\text{ION}}}{NkT} \quad (4)$$

where A^{IDEAL} is the ideal contribution and $A^{\text{MONO.}}$, $A^{\text{ASSOC.}}$, A^{CHAIN} , and A^{ION} are the contributions to the free energy due to monomer–monomer interactions, intermolecular association, chain formation, and ionic interactions, respectively.

3.1. Ideal Contribution. In the case of a four-component mixture the ideal contribution is given by⁶⁸

$$\frac{A^{\text{IDEAL}}}{NkT} = \left(\sum_{i=1}^4 x_i \ln \rho_i \Lambda_i^3 \right) - 1 \quad (5)$$

where N is the number of molecules, k Boltzmann's constant, T the temperature, x_i the mole fraction, $\rho_i = N_i/V$ the number density (V is the total volume), and Λ_i the thermal de Broglie wavelength of component i .

3.2. Monomer Contribution. In the SAFT-VR approach the contribution to the free energy due to monomer–monomer interactions is given by a second-order high-temperature expansion using a square-well potential to model the monomer–monomer interactions.⁴³ In the case of a four-component system it can be written as

$$\begin{aligned} \frac{A^{\text{MONO}}}{NkT} &= \left(\sum_{i=1}^4 x_i m_i \right) a^{\text{MONO}} \\ &= \left(\sum_{i=1}^4 x_i m_i \right) \left(a^{\text{HS}} + \frac{1}{kT} a_1 + \frac{1}{(kT)^2} a_2 \right) \end{aligned} \quad (6)$$

where m_i is the number of spherical segments of component i ($m_1 = 1$, $m_2 = (C - 1)/3 + 1$, $m_3 = 1$, and $m_4 = 1$) and $a^{\text{MONO}} = A^{\text{MONO}}/(N_s kT)$ is the monomer free energy per segment (N_s is the total number of segments in the mixture). a^{HS} is the hard-sphere free energy contribution as given by the equation of Boublik⁶⁹ and Mansoori et al.,⁷⁰

$$a^{\text{HS}} = \frac{6}{\pi \rho_s} \left[\left(\frac{\zeta_2^3}{\zeta_3^2} - \zeta_0 \right) \ln(1 - \zeta_3) + \frac{3\zeta_1 \zeta_2}{1 - \zeta_3} + \frac{\zeta_2^3}{\zeta_3(1 - \zeta_3)^2} \right] \quad (7)$$

where the reduced densities ζ_i are then defined as

$$\zeta_1 = \frac{\pi}{6} \rho_s \left[\sum_{i=1}^4 x_{s,i} (\sigma_{ii})^3 \right] \quad (8)$$

where $x_{s,i}$ is the mole fraction of segments of type i given by

$$x_{s,i} = \frac{m_i x_i}{\sum_{k=1}^4 m_k x_k} \quad (9)$$

The mean attractive energy a_1 of the mixture is the sum of the terms of each pair interaction

$$a_1 = \sum_{i=1}^4 \sum_{j=1}^4 x_{s,i} x_{s,j} a_1^{ij} \quad (10)$$

and, since in this work no ion–ion or ion–oil square-well interactions are taken into account, it is given by

$$a_1 = x_{s,1}^2 a_1^{11} + x_{s,2}^2 a_1^{22} + 2x_{s,1} x_{s,2} a_1^{12} + 2x_{s,1} x_{s,3} a_1^{13} + 2x_{s,1} x_{s,4} a_1^{14} \quad (11)$$

To study the global phase behavior in these systems, we use the van der Waals one-fluid mixing rule with respect to the radial distribution function of the reference hard-sphere system so that each of the i – j contributions of the mean attractive energy is given as

$$a_i^{ij} = -\rho_s \alpha_{ij}^{\text{VDW}} g_0^{\text{HS}}[\sigma_x; \zeta_x^{\text{eff}}(\zeta_x; \lambda_{ij})] \quad (12)$$

where the van der Waals attractive parameter for a square-well segment of range λ_{ij} and depth ϵ_{ij} is obtained as

$$\alpha_{ij}^{\text{VDW}} = \frac{2\pi}{3} \epsilon_{ij} \sigma_{ij}^3 (\lambda_{ij}^3 - 1) \quad (13)$$

and the contact radial distribution function is

$$g_0^{\text{HS}}[\sigma_x; \zeta_x^{\text{eff}}(\zeta_x; \lambda_{ij})] = \frac{1 - \zeta_x/2}{(1 - \zeta_x)^3} \quad (14)$$

In the van der Waals one-fluid mixing rule the diameter of the hypothetical fluid to which the mixture is mapped is given by

$$\sigma_x^3 = \sum_{i=1}^4 \sum_{j=1}^4 x_{s,i} x_{s,j} \sigma_{ij}^3 \quad (15)$$

which gives a van der Waals one-fluid definition of the packing fraction of the mixture as

$$\zeta_x = \frac{\pi}{6} \sigma_x^3 \rho_s \quad (16)$$

The nonconformal properties of the fluids are, however, retained in the calculation of the effective packing fraction, which is obtained as

$$\zeta_x^{\text{eff}}(\zeta_x; \lambda_{ij}) = c_1(\lambda_{ij}) \zeta_x + c_2(\lambda_{ij}) \zeta_x^2 + c_3(\lambda_{ij}) \zeta_x^3 \quad (17)$$

where the c_1 , c_2 , and c_3 constants are given in ref 43. Equations 12–17 correspond to mixing rule MX1b as detailed in ref 44. It is more convenient to use the one-fluid approximation in global studies of the phase behavior, the expressions are somewhat simpler than in the higher order approximations, and they allow the calculation of the critical properties while a similar level of accuracy away from the critical points is obtained.

The fluctuation term in the attractive free energy of the mixture is obtained from each of the i – j contributions as

$$a_2 = \sum_{i=1}^4 \sum_{j=1}^4 x_{s,i} x_{s,j} a_2^{ij} \quad (18)$$

and, as before, no ion–ion or ion– n -alkane terms are incorporated so that

$$a_2 = x_{s,1}^2 a_2^{11} + x_{s,2}^2 a_2^{22} + 2x_{s,1} x_{s,2} a_2^{12} + 2x_{s,1} x_{s,3} a_2^{13} + 2x_{s,1} x_{s,4} a_2^{14} \quad (19)$$

In the SAFT-VR approach the local compressibility approximation is used for each of the a_2^{ij} terms,⁷¹

$$a_2^{ij} = \frac{1}{2} K^{\text{HS}} \epsilon_{ij} \rho_s \frac{\partial a_1^{ij}}{\partial \rho_s} \quad (20)$$

and K^{HS} is the isothermal compressibility given by the Percus–Yevick expression (see ref 43 and references therein).

For the sake of clarity it is important to re-iterate here that in this work we have used the van der Waals one-

fluid approximation to describe the mixture contributions of the mean attractive energy and the fluctuation term. This approximation corresponds to mixing rule M1Xb in ref 44. In addition, the ion–ion and ion–oil attractive square-well energies (ϵ_{33} , ϵ_{44} , ϵ_{23} , ϵ_{24} , ϵ_{34}) are all zero.

3.3. Association Contribution. The free energy contribution due to the association of s_i sites in a four-component mixture can be obtained from the thermodynamic perturbation theory of Wertheim^{72–77} as

$$\frac{A^{\text{ASSOC.}}}{NkT} = \sum_{i=1}^4 x_i \left[\sum_{a=1}^{s_i} \left(\ln X_{a,i} - \frac{X_{a,i}}{2} \right) + \frac{s_i}{2} \right] \quad (21)$$

where the first sum is over the number of species and the second over the number of sites s_i of a given type. In this work only the water molecules are modeled as associating. Each of the sites is modeled in the same way so that four site–site equivalent interactions are possible between the water molecules; in this way, the free energy of association can be written as

$$\frac{A^{\text{ASSOC.}}}{NkT} = x_1 [4 \ln X_1 - 2X_1 + 2] \quad (22)$$

where X_1 is the fraction of water molecules not bonded at a given site. It is given by the mass action equations as

$$X_1 = \frac{1}{1 + 2x_1 \rho \Delta_{11}} \quad (23)$$

where Δ_{11} is written as a function of the bonding volume available for the water sites,⁷⁶ the Mayer f -function of the water–water site–site interaction $F_{11} = \exp(\epsilon_{11}^{\text{HB}}/kT) - 1$, and the contact radial distribution function of the water square-well segments in the mixture $g^{\text{M}}(\sigma_{11}; \zeta_3)$ as

$$\Delta_{11} = K_{11} F_{11} g^{\text{M}}(\sigma_{11}; \zeta_3) \quad (24)$$

The radial distribution function of the monomer system is obtained from the high-temperature expansion as

$$g^{\text{M}}(\sigma_{11}; \zeta_3) = g^{\text{HS}}(\sigma_{11}; \zeta_3) + \frac{\epsilon_{11}}{kT} g_1(\sigma_{11}; \zeta_3) \quad (25)$$

where $g^{\text{HS}}(\sigma_{11}; \zeta_3)$ is the contact radial distribution function of the reference hard-sphere mixture as given by the expression of Boubik⁶⁹ and Mansoori et al.⁷⁰ The first perturbation term $g_1(\sigma_{11}; \zeta_3)$ is obtained from the Clausius virial theorem and the density derivative of the Helmholtz free energy (see ref 43 for more details).

It should be noted that although we consider only one associating component in the mixture, the equation of state is general, and more associating compounds can be incorporated. For example, association interactions between water and ions have been treated in a recent work.³⁸

3.4. Chain Contribution. Within the thermodynamic perturbation theory of Wertheim a simple expression is obtained for the contribution to the free energy due to the formation of chain molecules of tangentially bonded monomers. The expression is given in terms of the contact radial distribution function of the monomers and the number of monomer–monomer contacts as⁷⁸

$$\frac{A^{\text{CHAIN}}}{NkT} = - \sum_{i=1}^4 x_i (m_i - 1) \ln g^M(\sigma_{ii}) \quad (26)$$

In this work only the n -alkane molecules are chainlike so that

$$\frac{A^{\text{CHAIN}}}{NkT} = -x_2(m_2 - 1) \ln g^M(\sigma_{22}) \quad (27)$$

and the contact radial distribution function can be obtained using eq 27 as in the previous section.

3.5. Ionic Contribution. The contribution to the free energy due to the Coulombic interactions in the mixture is obtained in an approximate way using the solution of the restricted primitive model (RPM) in the mean spherical approximation (MSA). In the RPM the anion and cation are modeled as hard spheres of equal diameter $\tilde{\sigma}$ interacting through a uniform medium of dielectric constant D . The pair potential for the i - j ion-ion interaction is given by⁴

$$u_{ij}(r) = \begin{cases} +\infty & \text{if } r \leq \tilde{\sigma} \\ (z_i z_j e^2)/(Dr) & \text{if } r > \tilde{\sigma} \end{cases} \quad (28)$$

where z_i is the charge of ion i and e is the unit electrostatic charge ($e = 4.8 \times 10^{-10}$ esu). The hard-sphere diameter $\tilde{\sigma}$ used to model the ionic species in the RPM is given by the average of the ionic diameters;³⁷ in this work 1:1 salts are always considered so that

$$\tilde{\sigma} = \frac{\sigma_{33} + \sigma_{44}}{2} \quad (29)$$

Waisman and Lebowitz⁷⁹ were able to solve the Ornstein-Zernike equation for this model using the mean spherical closure; in this approximation the ionic contribution to the free energy is obtained as⁴

$$\frac{A^{\text{IONS}}}{NkT} = - \frac{3x^2 + 6x + 2 - 2(1 + 2x)^{3/2}}{12\pi\rho\tilde{\sigma}^3} \quad (30)$$

where $x = \kappa\tilde{\sigma}$, and

$$\kappa^2 = \frac{4\pi e^2}{DkT} \sum_{j=1}^{\tilde{n}} \rho_j z_j^2 \quad (31)$$

is the inverse Debye length, and the sum is over the number of ionic species \tilde{n} only, so that in this work

$$\kappa^2 = \frac{4\pi e^2}{DkT} (\rho_3 z_3^2 + \rho_4 z_4^2) \quad (32)$$

In a previous work³⁸ we discussed the use of a number of approximations which can be implemented equally easily within this framework. In particular, we observed that the original Debye-Hückel approach can provide a good description of the phase behavior of electrolyte solutions if combined with an accurate model for water, although better agreement for the density of the solutions is generally obtained with the MSA, as in this case the ionic sizes are explicitly incorporated.

As mentioned in the previous section, the dielectric constant D takes the experimental value of pure water at each temperature. In a previous work Wu and Prausnitz²⁷ have proposed an expression for the dielectric in the mixture, which is a function of the water

dielectric constant and the composition of the mixture, together with an adjustable constant characteristic of each hydrocarbon. The marked immiscibility in this system, however, means that in the water-rich phase the result is essentially the dielectric constant of water, and in this way there is no need to add an extra adjustable parameter in the calculation. Recall also that, as mentioned in the previous section, we assume the oil-rich phase and the vapor phase (if present) to be salt free.

3.6. Phase Coexistence Conditions. Once the Helmholtz free energy is determined, standard thermodynamic relations can be used to obtain other thermodynamic properties.¹⁰ Phase equilibria between n phases requires that the temperature, pressure, and chemical potentials of all the components in all of the phases be equal, that is,

$$\begin{aligned} T^{\text{I}} &= T^{\text{II}} = \dots = T^n \\ p^{\text{I}} &= p^{\text{II}} = \dots = p^n \\ \mu_i^{\text{I}} &= \mu_i^{\text{II}} = \dots = \mu_i^n \end{aligned} \quad (33)$$

In this work we consider a number of binary water + n -alkane mixtures and of four-component (water + n -alkane + anion + cation) mixtures. It is useful to consider in more detail the conditions for equilibria in the case of the mixtures involving the ionic species. The Gibbs phase rule indicates that, in a four-component system, a maximum of five phases can be found in equilibrium. Although salt-induced phase separation can be observed in concentrated aqueous solutions, we do not expect such a separation to occur here. We take into account a maximum of three phases (as expected in the water + n -alkane systems); hence, assuming that while the ionic components will modify the equilibrium compositions, they will not induce separation into new phases. In addition to this the ionic species are present only in the water-rich liquid phase, so the equilibrium conditions are given by

$$\begin{aligned} T^{\text{W}} &= T^{\text{O}} = T^{\text{g}} \\ p^{\text{W}} &= p^{\text{O}} = p^{\text{g}} \\ \mu_1^{\text{W}} &= \mu_1^{\text{O}} = \mu_1^{\text{g}} \\ \mu_2^{\text{W}} &= \mu_2^{\text{O}} = \mu_2^{\text{g}} \end{aligned} \quad (34)$$

where W refers to the water-rich liquid phase, O to the oil-rich liquid phase, and g to the gas (vapor) phase. In addition to the phase equilibria conditions, the condition of electroneutrality must also be satisfied. In the case of 1:1 electrolytes this means that the mole fraction of anions and cations must be equal, that is,

$$x_3^{\text{W}} = x_4^{\text{W}} \quad (35)$$

Equations 34 and 35 are solved using a Marquat-Levenberg method.⁸⁰ It is worth noting that it is more convenient to solve the expressions in terms of reduced variables $T^* = kTb_{11}/\alpha_{11}^{\text{VDW}}$, $p^* = pb_{11}^2/\alpha_{11}^{\text{VDW}}$, and $\mu^* =$

Table 1. SAFT-VR Parameters for Pure Nonionic Components^a

substance	<i>m</i>	$\sigma/\text{\AA}$	λ	$(\epsilon/k)/\text{K}$	$(\epsilon^{\text{HB}}/k)/\text{K}$	$K/\text{\AA}^3$
water	1	3.036	1.8	253.3	1366	1.028
methane	1	3.6847	1.4479	167.3	0	0
<i>n</i> -hexane	2.667	3.92	1.552	250.4	0	0
<i>n</i> -decane	4	3.967	1.592	247.1	0	0

^a *m* is the number of square-well segments in the molecule, σ is the hard-core diameter, and λ and ϵ are the range and depth of the attractive square-well potential. In the case of associating molecules, such as water, ϵ^{HB} is the site–site interaction energy and *K* the bonding volume. *k* is the Boltzmann constant.

Table 2. Pauling Ionic Diameters σ_{ij} and Optimized SAFT-VR Water–Ion Interaction Parameters Where $\sigma_{1j} = (\sigma_{11} + \sigma_{ij})/2$ Is the Unlike Hard-Sphere Diameter and ϵ_{1j} and λ_{1j} Are the Square-Well Depth and Range of the Water–Ion Attractive Interaction^a

ion	$\sigma_{ij}/\text{\AA}$	$\sigma_{1j}/\text{\AA}$	$(\epsilon_{1j}/k)/\text{K}$	λ_{1j}	α_{1j}^{VDW}
Li ⁺	1.36	2.198	2348.17	1.2	0.53
Na ⁺	1.9	2.468	970.2	1.2	0.31
K ⁺	2.66	2.848	631.36	1.2	0.31
Cl [−]	3.62	3.328	395.68	1.2	0.31
Br [−]	3.92	3.478	447.31	1.2	0.4
I [−]	4.4	3.718	457.7	1.2	0.5

^a $\alpha_{1j}^{\text{VDW}} = 2\pi/3\sigma_{1j}^3\epsilon_{1j}(\lambda_{1j}^3 - 1)$ is the integrated water–ion dispersion energy. Note the typographical error in ref 37.

μ/kT , where $b_{11} = (\pi/6)\sigma_{11}^3$, and reduced parameters $\sigma_{ij}^* = \sigma_{ij}/\sigma_{11}$, $\alpha_{ij}^* = \alpha_{ij}/\alpha_{11}$, $\epsilon_{11}^{\text{HB}} = \epsilon_{11}^{\text{HB}} b_{11}/\alpha_{11}$, and $K^* = K_{11}/\sigma_{11}^3$.

4. Results and Discussion

The effect of the addition of salt on the phase behavior of water + *n*-alkane mixtures is studied using the SAFT-VRE approach presented in the previous section. We treat the approach as a predictive tool whenever possible, determining the unlike intermolecular parameters which characterize the binary water–*n*-alkane and water–ion interactions by comparison with experimental data, but no additional adjustable parameters are used to study the water + *n*-alkane + salt systems. We show that the approach provides an excellent description of the salting-out effect as compared to experimental data. The extreme degree of immiscibility characteristic of these systems means that few experimental data are available, which makes predictive approaches especially useful. We examine first the phase behavior of a water + methane + NaCl mixture as some experimental data of the methane solubility are available for this system.^{53,54} The comparison of the theoretical predictions and experiments provide an indication of the accuracy of the proposed framework. We then predict the salting-out effect of other strong electrolytes. The phase behavior of aqueous solutions of longer *n*-alkanes is studied later. We have considered in particular the water *n*-hexane and water + *n*-decane systems, examining the mutual water–oil solubilities in the three-phase region in the presence of added salts.

We have already presented in previous works the optimized SAFT-VR and SAFT-VRE parameters for all of the pure components considered here (see section 2 of this work and refs 37, 43, and 64 for more details). We have collected the parameters in Tables 1 and 2 for completeness.

4.1. Water + Methane + Salt. As mentioned earlier, mixtures of water + *n*-alkanes are characterized by a

marked degree of immiscibility. In the classification of Scott and van Konynenburg,^{81,82} a mixture of water + methane exhibits a so-called type-III phase behavior. In the *pT* projection of the phase diagram the vapor–liquid critical line appears in two branches: starting from the critical point of water (component 1), the vapor–liquid critical line continues to high pressures, merging into the liquid–liquid critical line, where the critical points correspond to states involving two phases of liquidlike density; at low pressures and temperatures, a second, small, critical line is found which starts at the critical point of pure methane (component 2) and finishes at a so-called upper-critical end point (maximum pressure at which three phases are found in coexistence). Using the SAFT-VR approach we are able to predict this type of phase behavior using the Lorentz–Berthelot combining rule for the unlike intermolecular parameters; that is, with $k_{ij} = 0$ and $\gamma_{ij} = 0$ in eqs 1 and 2. This provides an indication of the extent to which nonidealities are already incorporated in the model. However, to carry out a quantitative study of the salting out, it is convenient to obtain the best possible description of the methane compositions in the water-rich phase. We find that by using $k_{ij} = 0$ and $\gamma_{ij} = 0$, we slightly overpredict the extent of immiscibility in the mixture at the conditions of interest (*T* = 398 and 443 K). By comparing with the experimental data at these conditions, we find that the best description is obtained using $k_{ij} = -0.00967$ and $\gamma_{ij} = -0.05576$ (see also Table 2). It may seem unusual at first inspection to observe that these unlike adjustable parameters are negative and not positive as could be expected. The SAFT model for water + *n*-alkane mixtures incorporates water–water hydrogen-bonding interactions, and it takes into account the chainlike nature of the *n*-alkane molecules. These two factors result in the approach predicting liquid–liquid phase separation, even in the case where no adjustable cross-interaction parameters are involved; this highlights the accuracy of the model. Similar results are obtained using detailed computer simulations. Errington et al.⁸³ have performed Gibbs ensemble Monte Carlo simulations using an extended version of the simplified point charge model for water (SPC/E) and the united atom model of Smit, Karaborni, and Siepmann^{84,85} for the *n*-alkanes molecules. In particular, they calculate the phase behavior of a mixture of water + methane in the same conditions as we consider here and find that the simulation data slightly overpredict the extent of immiscibility when compared to the experimental data. Using the optimized cross-interaction parameters $k_{ij} = -0.00967$ and $\gamma_{ij} = -0.05576$, an accurate description of the methane compositions in the water-rich phase is obtained, and we have also confirmed that the global phase behavior of the mixture is well-described. In Figure 3 the *pT* projection of the *pTx* surface for the water + methane mixture is presented; as can be clearly seen, the mixture exhibits a type-III phase behavior in the classification of Scott and van Konynenburg. An overprediction of the critical points of the pure components can be noticed; this is expected for a classical equation of state such as SAFT. Starting from the critical point of water, the critical curve of the mixture is obtained in good overall agreement with the experimental data.^{86–89} The study of the isothermal *px* slices of the phase diagram shows that a good description of the phase behavior is also given in terms of composition using these parameters (see Figure 4).

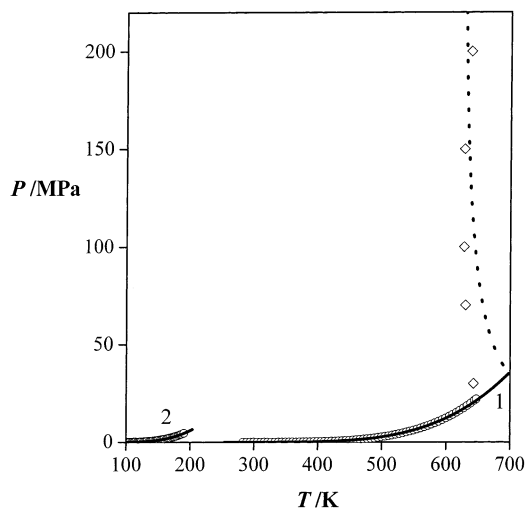


Figure 3. pT projection of the pTx phase diagram for water (1) + methane (2) compared with the SAFT-VR predictions. The solid curves correspond to the calculated pure component vapor pressures and the dotted curve to the critical line. The open circles correspond to the pure component experimental vapor pressures^{67,90} and the diamonds to the high-temperature critical pressures.^{86–89}

As mentioned, the determination of the unlike parameters was carried out placing special emphasis on the description of the methane-in-water compositions at temperatures $T = 398$ and 443 K, as these provide

the baseline to consider the effect of added salts. In Figure 5 the methane solubility in pure water and in aqueous electrolyte solutions of varying molality are shown compared to experimental data. The calculations are obtained using the same unlike intermolecular parameters for water + methane as in the previous figures, the water-ion interactions are modeled using the parameters determined in a previous work³⁷ (see also Table 2), and no ion-methane adjustable parameters are used as no dispersion interaction between these species is incorporated. The salting-out effect caused by the addition of NaCl to the water + methane mixture is evident in the figures. The solubility of methane in water decreases as the salt concentration increases. In our study of the isotherms at 398.15 K (125 °C), a 50% reduction in the amount of methane in water is achieved with a NaCl solution of concentration 4 m at a constant pressure of 50 MPa. It is clearly seen that the predictions of the theory are in very good agreement with the experimental data. At the higher temperature of 443.15 K (170 °C) higher concentrations of methane are found in the water-rich phase as indicated by the experimental data and SAFT-VR calculations. Together with this, the salting-out effect observed for the addition of NaCl is less marked in these conditions; a solution 5.2 m in NaCl induces a reduction of only 33% of the methane present in water at the same pressure of 50 MPa. The agreement between the experimental data and the predictions of our approach is remarkable in

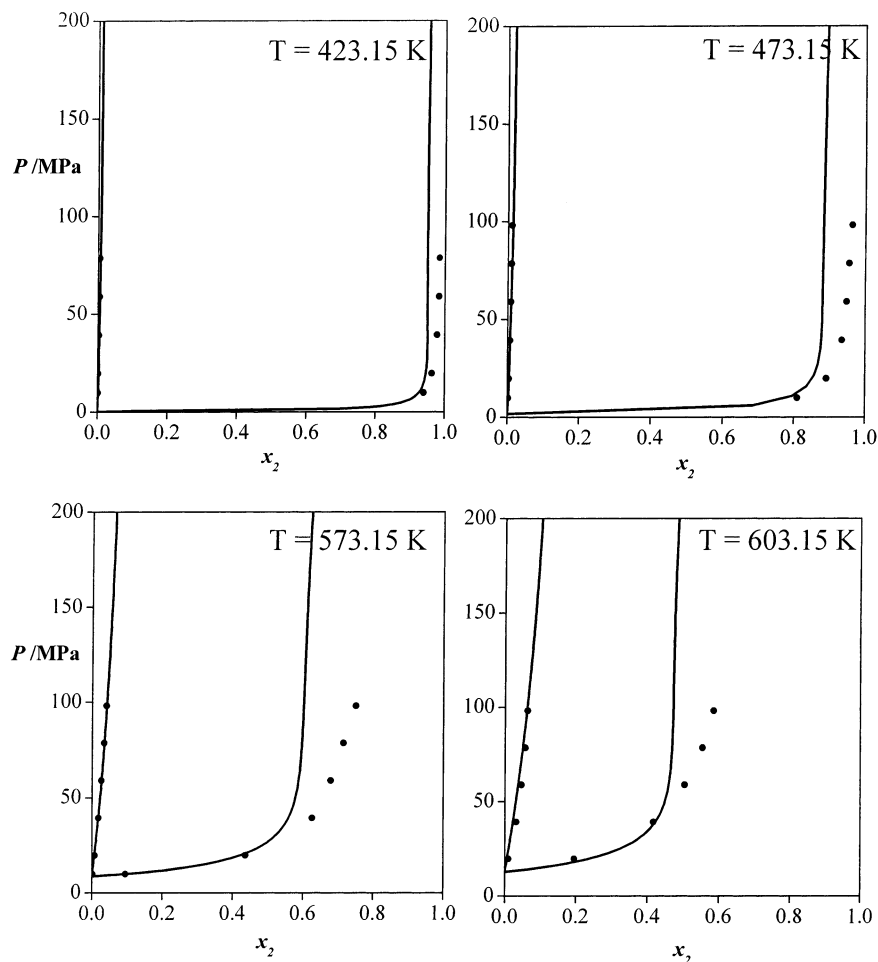


Figure 4. Constant temperature Px slices for water (1) + methane (2) compared with SAFT-VR calculations. The filled circles correspond to the experimental values of the coexisting compositions of the two phases⁹¹ and the curves to the theoretical calculations. x_2 corresponds to the methane mole fraction.

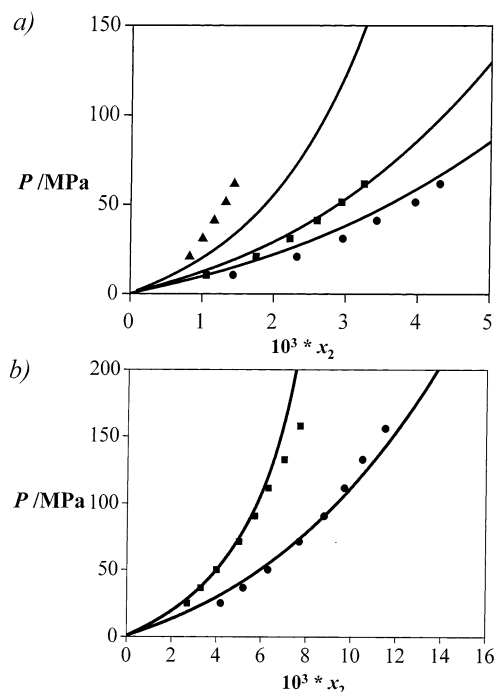


Figure 5. The salting out of methane by NaCl is seen in two temperature P - x slices for water (1) + methane (2) at (a) 398.15 K (125 °C) and (b) 443.15 K (170 °C) where only the compositions of methane in the water-rich phase are shown. The symbols correspond to the experimental data^{26,54,92} and the curves to the SAFT-VRE predictions. In (a) the filled circles correspond to the methane coexistence compositions in the case of a mixture without salt, the squares to the compositions in a mixture of water + methane + 1 m NaCl, and the triangles to the methane compositions in the case of water + methane + 4 m NaCl. In (b) the filled circles correspond to the methane coexistence compositions in the case of a mixture without salt and the squares to the methane compositions in a mixture of water + methane + 9.4 wt % (5.2 m) NaCl. x_2 corresponds to the methane mole fraction.

this case. Note that the experimental data are used only to assess the accuracy of the theoretical approach and not to determine the unlike intermolecular parameters. The water–ion interaction parameters were determined in a previous work in which we studied the vapor pressure depletion in aqueous solutions of strong electrolytes;³⁷ the same parameters are used in this work (see Table 2, noting the typographical error in Table 1 of ref 37). No extra adjustable parameters are needed to predict the salting out of methane by NaCl. It is worth noting the small scale of the figures.

Encouraged by these results, we have also examined the salting-out effect of other electrolyte solutions. In a previous work³⁷ a table of ionic and water–ion intermolecular parameters was presented; using those parameters, we predict the change in the solubility of methane at constant temperature 398.15 K when other salts are added to the aqueous solution. The importance of the cation is studied by comparing the salting out obtained with the chlorine salts in Figure 6a and in Figure 6b the importance of the anion is considered by studying three sodium salts. A 4 m electrolyte solution is considered in each case, and the solubility of methane in water without added salt is also presented for comparison. In the case of a changing cation it is clear that a dramatic salting out of methane can be achieved using a solution of LiCl. At 50 MPa the composition of methane in pure water is 3.58×10^{-3} in mole fraction, while if LiCl is added to the mixture, the amount of

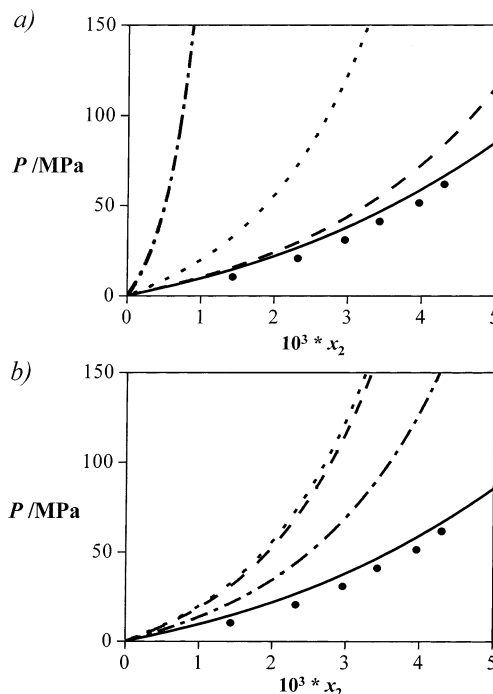


Figure 6. (a) Salting out of methane by LiCl (dashed–dotted curve), NaCl (short-dashed curve), and KCl (long-dashed curve) at 398.15 K (125 °C) predicted with the SAFT-VRE approach. (b) Salting out of methane by NaCl (short-dashed curve), NaBr (long-dashed curve), and NaI (dashed–dotted curve) at 398.15 K (125 °C) predicted with the SAFT-VRE approach. The salt concentration is 4 m in all cases. In both figures the experimental^{26,54,92} (filled circles) and calculated (solid curves) coexistence compositions of methane in the water-rich phase for the case of a mixture of water + methane with no salt are also presented for comparison. x_2 corresponds to the methane mole fraction.

methane found in the aqueous phase is 0.5×10^{-3} . On the other hand, using the same amount of KCl results in a poor salting out of methane. At 50 MPa the amount of methane soluble in water + 4 m KCl is predicted to be 3.24×10^{-3} in mole fraction. It is worth noting that Li^+ is the ion of smallest diameter and it was modeled as having a very strong attractive interaction with water. K^+ is the largest of the cations and has the weakest interaction with water. In the examination of the salting out of methane with sodium salts, it is found that the most effective separation is achieved in the case of the NaCl solution (see Figure 6b). At 50 MPa the methane content in the water-rich phase is 1.87×10^{-3} in mole fraction when a solution 4 m in NaCl is used; in the case of a 4 m solution of NaI the methane content is 2.50×10^{-3} , as compared to a mole fraction of 3.58×10^{-3} found in the case of pure water.

In Figures 7 and 8 we examine in more detail the effect of the added salts in relation to the fraction of water molecules which are hydrogen-bonded and the density of the water-rich phase. We examine first the three mixtures of methane with aqueous solutions 4 m in chlorine salts (LiCl, NaCl, and KCl) at a temperature of 398.15 K (Figure 7). More than 99% of water molecules are found to be forming at least one hydrogen bond in the water phase. More interestingly, our calculations suggest that although salting out (a decrease in the solubility of methane in water) is seen in the case of the three chlorine salts, KCl and NaCl cause a decrease in the number of water molecules bonded, while adding LiCl increases the number of water molecules hydrogen-bonded. Note that, in our proposed

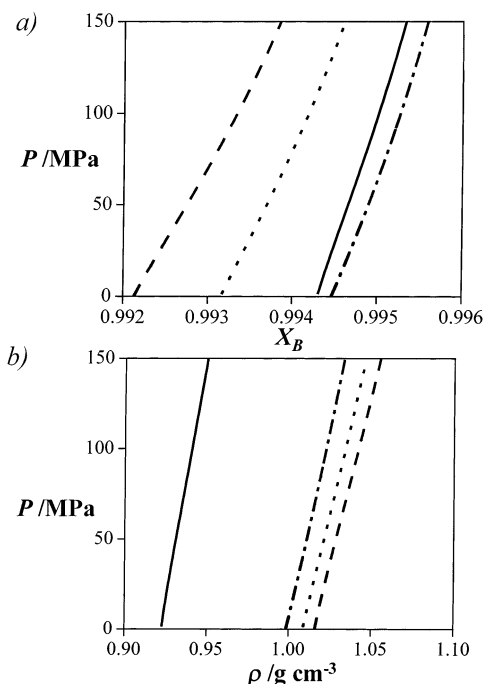


Figure 7. (a) Calculated fractions X_B of water molecules bonded at at least one site in the water-rich phase and (b) densities ρ of the water-rich phase for mixtures of water + methane with no added salt (solid curve), water + methane + 4 m LiCl (dotted-dashed curve), water + methane + 4 m NaCl (short-dashed curve), and water + methane + 4 m KCl (long-dashed curve) at 398.15 K (125 °C).

model, attractive water–ion dispersion energies are incorporated in all cases, but no water–ion association is taken into account. It is likely that the increase in the fraction of water molecules that are bonded seen in the case of the LiCl solution is due to the marked salting out of methane in this case. It is generally expected that the presence of the ions would disrupt the network of hydrogen bonds (as seen for NaCl and KCl), but the dramatic decrease in the amount of methane present when LiCl is added to the mixture means that more water–water hydrogen bonds can be formed. The expected increase in the density of the water-rich phase when salts are added can also be clearly seen in the figure. The smallest density change is seen in the case of LiCl, as would correspond to the smallest of the ions considered. Similar calculations are carried out for the series of sodium salts (NaCl, NaBr, and NaI) in Figure 8. In this case, the addition of salt to the water + methane mixture results in a decrease of hydrogen bonding between water molecules, as could be expected by comparison with Figure 7, and a marked increase in density is seen, as corresponds to the larger sizes of the ions in these salts.

4.2. Water + *n*-Alkane + Salt. The approach presented can also be used to study the solubility of long-chain alkanes in water and the effect of the added salts in solution. The solubility of water in *n*-alkanes have been of interest for some time due to their importance in the design of many refining and petrochemical processes, while the solubility of alkanes in water is of interest in environmental control. While both are very small, it is interesting to note that the solubility of the oil in water is orders of magnitude lower than the solubility of water in the alkane. In addition to this, an anomalous increase in the solubility of the alkane in

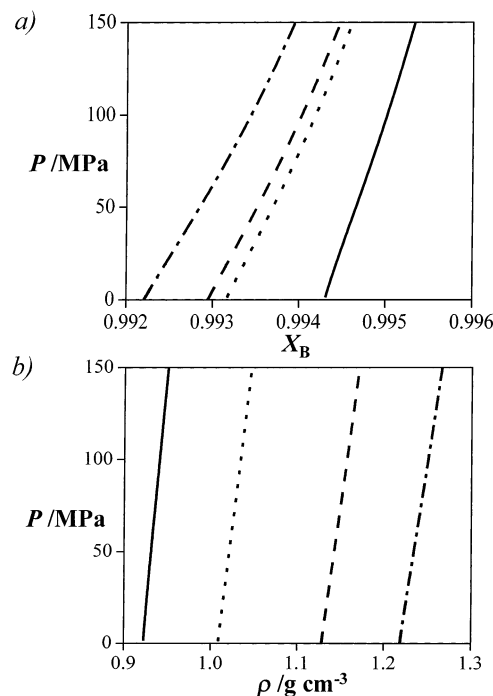


Figure 8. (a) Calculated fractions X_B of water molecules bonded at at least one site in the water-rich phase and (b) densities ρ of the water-rich phase for mixtures of water + methane with no added salt (solid curve), water + methane + 4 m NaCl (short-dashed curve), water + methane + 4 m NaBr (long-dashed curve), and water + methane + 4 m NaI (dashed-dotted curve) at 398.15 K (125 °C).

water is observed at low temperature. A number of sophisticated equations of state incorporating associating models for the water molecules have been used to model this phase behavior rather successfully.^{50–52} In all of the cases it is found that it is difficult to predict accurately both the water solubility and the oil solubility and that the anomalous increase in the alkane solubility cannot be reproduced. In our present work we do not intend to provide an in-depth investigation of water + alkane association models. We have concentrated on reproducing the oil-in-water solubility and the anomalous increase in this solubility seen at low temperatures, to the detriment of the water-in-oil solubilities, as we are interested in observing salting-out effects. We find that it is possible to reproduce the anomalous solubility by using two adjustable parameters k_{ij} and γ_{ij} , which determine the strength of the unlike dispersion interaction; in this case $k_{ij} = -0.74165$ and $\gamma_{ij} = 0.22043$. We are also interested in providing a predictive framework to model these mixtures, and so we have performed calculations studying the mutual solubilities for the series of *n*-alkanes from *n*-hexane to *n*-dodecane and find good agreement in all cases using these parameters. In this work we consider the solubility of *n*-hexane and *n*-decane in water as examples.

The mutual solubilities of water and oil along the three-phase (liquid–liquid–vapor) line are presented in Figures 9 and 10. It is evident from the figures that the solubility of water in oil is orders of magnitude higher than the solubility of oil in water. As can be expected the solubility of water in oil increases with increasing temperature. More unexpected, however, is the decrease in the solubility of the oils in water as the temperature is increased between 273 and 325 K; as the temperature is increased further, the expected increase in solubility

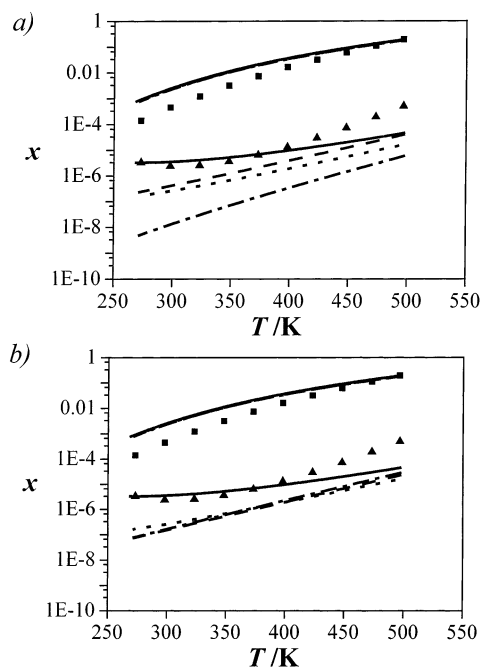


Figure 9. Coexistence compositions x of the liquid water-rich and n -alkane-rich phases for increasing temperatures T along the three-phase line in mixtures of water + n -hexane and water + n -hexane + salt. In (a) the dashed-dotted curve corresponds to the calculated compositions for a mixture of water + n -hexane + 2 m LiCl, the short-dashed curve to those of a mixture of water + n -hexane + 2 m NaCl, and the long-dashed curve to those of a mixture of water + n -hexane + 2 m KCl. In (b) the short-dashed curve corresponds to the calculated compositions for a mixture of water + n -hexane + 2 m NaCl, the long-dashed curve to those of a mixture of water + n -hexane + 2 m NaBr, and the dashed-dotted curve to those of a mixture of water + n -hexane + 2 m NaI. The symbols correspond to the experimental data⁹³ (triangles for the n -hexane-in-water compositions and squares for the water-in- n -hexane compositions) for a mixture with no added salt and the solid curves to the SAFT-VR calculations for a mixture of water + n -hexane with no added salt; these are presented for comparison.

is observed. This seems to indicate a tendency toward a lower critical solution temperature (LCST); that is, a lower limit in temperature at which oil and water would become miscible. Such phase behavior is usually associated with hydrogen-bonding mixtures, as it is believed that the increased miscibility is driven by the enthalpic contribution of unlike hydrogen bonds at low temperatures. In the case of the water + n -alkane mixtures, no hydrogen-bonding interactions occur between the two components (experimentally or theoretically) and so it is difficult to present arguments for this behavior. Using the SAFT-VR approach together with the optimized parameters showed that the solubilities are found to be in overall good agreement with the experimental data, and the anomalous behavior is reproduced. Unfortunately, we cannot provide an explanation for the behavior. We have considered other combinations of intermolecular unlike parameters that would also give rise to the increased miscibility of the oil and water and cannot, at this stage, reach any satisfactory conclusions, other than to point out that the unlike intermolecular parameters needed to reproduce this phase behavior with our approach suggest very large deviations from the usual arithmetic and geometrical mixing rules. It should be noted that the model for water selected in this work does not take into account dipolar interactions; it would be of interest to incorporate these into the treatment and to re-examine then the phase behavior

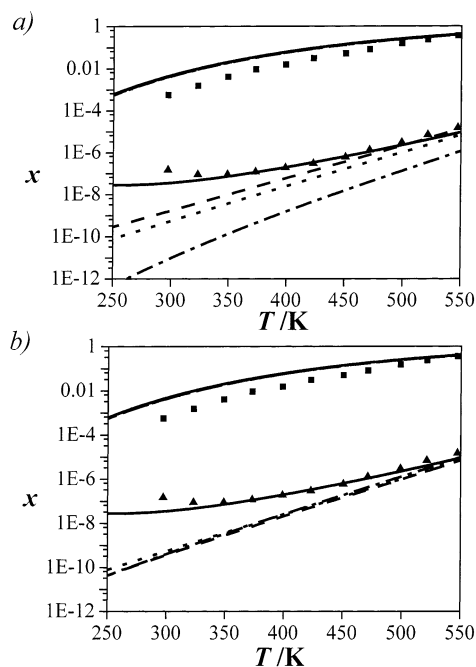


Figure 10. Coexistence compositions x of the liquid water-rich and n -alkane-rich phases for increasing temperature T along the three-phase line in mixtures of water + n -decane and water + n -decane + salt. In (a) the dashed-dotted curve corresponds to the calculated compositions for a mixture of water + n -decane + 2 m LiCl, the short-dashed curve to those of a mixture of water + n -decane + 2 m NaCl, and the long-dashed curve to those of a mixture of water + n -decane + 2 m KCl. In (b) the short-dashed curve corresponds to the calculated compositions for a mixture of water + n -decane + 2 m NaCl, the long-dashed curve to those of a mixture of water + n -decane + 2 m NaBr, and the dashed-dotted curve to those of a mixture of water + n -decane + 2 m NaI. The symbols correspond to the experimental data⁹³ (triangles for the n -decane-in-water compositions and squares for the water-in- n -decane compositions) for a mixture with no added salt and the solid curves to the SAFT-VR calculations for a mixture of water + n -decane with no added salt; these are presented for comparison.

of these mixtures. We plan to carry out this study in future work.

Within the framework presented it is possible to consider the effect of adding strong electrolytes to the water + n -alkane solutions. In Figures 9 and 10 the effect of the added salts can be seen for the case of aqueous solutions of n -hexane and n -decane, respectively; the electrolyte solutions considered are of concentration 2 m in each case. As can be seen in the figures, the amount of n -alkane present in the water-rich phase is reduced by orders of magnitude at low temperatures. Considering three chloride salts, the largest salting-out effect is achieved with LiCl, as in the case of the water + methane mixtures. A series of sodium salts with different anions is also considered, but little difference in salting out is observed between the different salts in these cases. It is also noticeable that, according to our calculations, the anomalous increase in oil solubility disappears when salt is added to the aqueous phase. LiCl is used commonly as a precipitating agent in the preparation of RNA and DNA; the dramatic decrease in the solubility of oils in water observed when LiCl is added to the mixtures suggests that this could provide a means to clean water of oil residues. It would be of much interest to be able to confirm the predictions of our calculations with experimental data.

5. Conclusions

The approach presented provides a simple way to model the salting out of nonpolar compounds from aqueous solutions. The salting out of *n*-alkanes is accurately predicted assuming the salt to be present only in the water-rich liquid phase, and hence, using only information of the water + *n*-alkane mixture and of the water + ion interactions. We have chosen to provide a global view of the phase behavior of these systems, rather than to accurately predict one specific region. Hence, we have used a set of transferable parameters for all the *n*-alkanes (except methane). Better accuracy of specific regions of the phase diagrams can be obtained by re-adjusting the unlike interaction parameters, although in such a case the predictive value of the approach is somewhat lost. Once the phase behavior of the water + *n*-alkane and water + salt systems is determined, we are able to truly predict the salting out of the *n*-alkane without requiring any experimental information of the water + *n*-alkane + salt system. In the case of aqueous solutions of methane + salt we have been able to compare the predictions of our approach with experimental data and find excellent agreement for the conditions of temperature and salt concentration considered. In the case of the solutions of larger *n*-alkanes salting out is also predicted, and the compositions of the *n*-alkane in the water phase are seen to be reduced by orders of magnitude. If our predictions are confirmed, this technique could be useful in water purification of oil traces. In the future we plan to extend the approach to consider polar compounds, which usually exhibit higher miscibility in water, such as alcohols and surfactants. A scheme needs to be devised to incorporate the dielectric constant of the two fluids. We are currently working in this area.

Acknowledgment

B.P. would like to thank the Engineering and Physical Sciences Research Council (EPSRC) and Schlumberger Cambridge Research for financial support, P.P. would like to thank BP for support, and A.G. acknowledges the EPSRC for the award of an Advanced Research Fellowship.

Literature Cited

- (1) Wecström, K.; Zulauf, M. Lower Consolute Boundaries of a Poly(oxyethylene) Surfactant in Aqueous Solutions of Monovalent Salts. *J. Chem. Soc., Faraday Trans. 1* **1985**, *81*, 2947.
- (2) Debye, P.; Hückel, E. Zur Theorie der Electrolyte. *Z. Phys.* **1923**, *24*, 185.
- (3) Debye, P.; Hückel, E. Zur Theorie der Electrolyte II. *Z. Phys.* **1923**, *24*, 305.
- (4) Lee, L. L. *Molecular thermodynamics of non-ideal Fluids*; Butterworths: Boston, 1988.
- (5) Adelman, S. A.; Deutch, J. M. Exact solution of the mean spherical model for strong electrolytes in polar solvents. *J. Chem. Phys.* **1974**, *60*, 3935.
- (6) Wei, D. Q.; Blum, L. Analytical solution of the mean spherical approximation for an arbitrary mixture of ions in a dipolar solvent. *J. Phys. Chem.* **1987**, *87*, 555.
- (7) Wu, R. S.; Lee, L. L. Vapor-liquid equilibria of mixed-solvent electrolyte solutions: ion-size effects based on the MSA theory. *Fluid Phase Equilib.* **1992**, *78*, 1.
- (8) Lee, L. L.; Lee, L. J.; Ghonasgi, D.; Llano-Restrepo, M.; Chapman, W. G.; Shukla, K. P.; Lomba, E. Theory and simulation for electrolyte solutions: applications to the phase equilibria of mixed solvent systems. *Fluid Phase Equilib.* **1996**, *116*, 185.
- (9) Lee, L. L. A molecular theory of Setchenov's salting-out principle and applications in mixed-solvent electrolyte solutions. *Fluid Phase Equilib.* **1997**, *131*, 67.
- (10) Prausnitz, J. M.; Lichtenthaler, R. N.; Gomes de Acevedo, E. *Molecular Thermodynamics of Fluid Phase Equilibria*; Prentice-Hall: Englewood Cliffs, NJ, 1986.
- (11) Cardoso, J. E. M.; O'Connell, J. P. Activity coefficients in mixed solvent electrolyte solutions. *Fluid Phase Equilib.* **1987**, *33*, 315.
- (12) Chen, C. C.; Britt, H. I.; Boston, J. F.; Evans, L. B. Part I: Single Solvent, Single Completely Dissociated Electrolyte Systems. *AIChE J.* **1982**, *28*, 588.
- (13) Chen, C. C.; Evans, L. B. A Local Composition Model for the Excess Gibbs Energy of Aqueous Electrolyte Systems. *AIChE J.* **1986**, *32*, 444.
- (14) Mock, B.; Evans, L. B.; Chen, C. C. Thermodynamic Representation of Phase Equilibria of Mixed-solvent Electrolyte Systems. *AIChE J.* **1986**, *32*, 1655.
- (15) Pitzer, K. S. Electrolytes. From dilute solutions to fused salts. *J. Am. Chem. Soc.* **1980**, *102*, 2902.
- (16) Zerres, H.; Prausnitz, J. M. Thermodynamics of Phase Equilibria in Aqueous-Organic Systems with Salt. *AIChE J.* **1994**, *40*, 676.
- (17) Kolker, A.; de Pablo, J. J. Thermodynamic modeling of concentrated multicomponent aqueous electrolyte and non-electrolyte solutions. *Chem. Eng. Sci.* **1995**, *50*, 1953.
- (18) Kolker, A.; de Pablo, J. J. Thermodynamic Modeling of Concentrated Aqueous Electrolyte and Nonelectrolyte Solutions. *AIChE J.* **1995**, *41*, 1563.
- (19) Kolker, A.; de Pablo, J. J. Thermodynamic Modeling of the Solubility of Salts in Mixed Aqueous-Organic Solvents. *Ind. Eng. Chem. Res.* **1996**, *35*, 228.
- (20) Sander, B.; Fredenslund, A.; Rasmussen, P. Calculation of vapour-liquid equilibria in mixed solvent/salt systems using an extended UNIQUAC equation. *Chem. Eng. Sci.* **1986**, *41*, 1171.
- (21) Stell, G.; Lebowitz, J. L. Equilibrium Properties of a System of Charged Particles. *J. Chem. Phys.* **1968**, *49*, 3706.
- (22) Henderson, D.; Blum, L.; Tani, A. Equation of State of Ionic Fluids. *Am. Chem. Soc. Symp. Ser.* **1985**, *300*, 28.
- (23) Chan, K. Y. Comparison of a primitive model perturbation theory with experimental data of simple electrolytes. *J. Phys. Chem.* **1990**, *94*, 8472.
- (24) Chan, K. Y. Ion-dipole model perturbation theory applied to simple electrolytes. *J. Phys. Chem.* **1991**, *95*, 7465.
- (25) Raatschen, W.; Harvey, A. H.; Prausnitz, J. M. Equation of state for solutions of electrolytes in mixed solvents. *Fluid Phase Equilib.* **1987**, *38*, 19.
- (26) Harvey, A. H.; Prausnitz, J. M. Thermodynamics of High-Pressure Aqueous Systems Containing Gases and Salts. *AIChE J.* **1989**, *35*, 635.
- (27) Wu, J.; Prausnitz, J. M. Phase Equilibria for Systems Containing Hydrocarbons, Water, and Salt: An Extended Peng-Robinson Equation of State. *Ind. Eng. Chem. Res.* **1998**, *37*, 1634.
- (28) Myers, J. A.; Sandler, S. I.; Wood, R. H. An Equation of State for Electrolyte Solutions Covering Wide Ranges of Temperature, Pressure, and Composition. *Ind. Eng. Chem. Res.* **2002**, *41*, 3282.
- (29) Jin, G.; Donohue, M. D. An equation of state for electrolyte solutions. 1. Aqueous systems containing strong electrolytes. *Ind. Eng. Chem. Res.* **1988**, *27*, 1073.
- (30) Jin, G.; Donohue, M. D. An equation of state for electrolyte solutions. 2. Single volatile weak electrolytes in water. *Ind. Eng. Chem. Res.* **1988**, *27*, 1737.
- (31) Jin, G.; Donohue, M. D. An equation of state for electrolyte solutions. 3. Aqueous solutions containing multiple salts. *Ind. Eng. Chem. Res.* **1991**, *30*, 240.
- (32) Economou, I. G.; Peters, C. J.; de Swaan Arons, J. Water-Salt Phase Equilibria at Elevated Temperatures and Pressures: Model Development and Mixture Predictions. *J. Chem. Phys.* **1995**, *99*, 6182.
- (33) Fürst, W.; Renon, H. Representation of Excess Properties of Electrolyte Solutions Using a New Equation of State. *AIChE J.* **1993**, *39*, 335.
- (34) Zuo, Y. X.; Fürst, W. Prediction of vapor pressure for nonaqueous electrolyte solutions using an electrolyte equation of state. *Fluid Phase Equilib.* **1997**, *138*, 87.
- (35) Zuo, Y. X.; Fürst, W. Use of an electrolyte equation of state for the calculation of vapor-liquid equilibria and mean activity

coefficients in mixed solvent electrolyte systems. *Fluid Phase Equilib.* **1998**, *150*, 267.

(36) Zuo, J. Y.; Zang, D.; Fürst, W. Extension of the electrolyte EOS of Fürst and Renon to mixed solvent electrolyte systems. *Fluid Phase Equilib.* **2000**, *175*, 285.

(37) Galindo, A.; Gil-Villegas, A.; Jackson, G.; Burgess, A. N. SAFT-VRE: Phase Behaviour of Electrolyte Solutions with the Statistical Associating Fluid Theory for Potentials of Variable Range. *J. Phys. Chem. B* **1999**, *103*, 10272.

(38) Gil-Villegas, A.; Galindo, A.; Jackson, G. A statistical associating fluid theory for electrolyte solutions (SAFT-VRE). *Mol. Phys.* **2001**, *99*, 531.

(39) Sengers, J. V.; Kayser, R. F.; Peters, C. J.; White, H. J. J. *Equations of state for fluids and fluid mixtures*; Elsevier: Holland, 2000.

(40) Vega, C.; MacDowell, L. G. Extending Wertheim's perturbation theory to the solid phase: The freezing of the pearl-necklace model. *J. Chem. Phys.* **2001**, *114*, 10411.

(41) Vega, C.; Blas, F. J.; Galindo, A. Extending Wertheim's perturbation theory to the solid phase of Lennard-Jones chains: Determination of the global phase diagram. *J. Chem. Phys.* **2002**, *116*, 7645.

(42) Blas, F. J.; Martín del Río, E.; de Miguel, E.; Jackson, G. An examination of the vapour-liquid interface of associating fluids using a SAFT-DFT approach. *Mol. Phys.* **2001**, *99*, 1851.

(43) Gil-Villegas, A.; Galindo, A.; Whitehead, P. J.; Mills, S. J.; Jackson, G.; Burgess, A. N. Statistical associating fluid theory for chain molecules with attractive potentials of variable range. *J. Chem. Phys.* **1997**, *106*, 4168.

(44) Galindo, A.; Davies, L. A.; Gil-Villegas, A.; Jackson, G. The thermodynamics of mixtures and the corresponding mixing rules in the SAFT-VR approach for potentials of variable range. *Mol. Phys.* **1998**, *93*, 241.

(45) Paricaud, P.; Galindo, A.; Jackson, G. Recent advances in the use of the SAFT approach in describing electrolytes, interfaces, liquid crystals and polymers. *Fluid Phase Equilib.* **2002**, *194*, 87.

(46) Liu, W. B.; Li, Y. G.; Lu, J. F. A new equation of state for real aqueous ionic fluids based on electrolyte perturbation theory, mean spherical approximation and statistical associating fluid theory. *Fluid Phase Equilib.* **1999**, *158*, 595.

(47) Li, X. S.; Lu, J. F.; Li, Y. G. Study on ionic surfactant solutions by SAFT equation incorporated with MSA. *Fluid Phase Equilib.* **2000**, *168*, 107.

(48) Fu, D.; Lu, J. F.; Bao, T. Z.; Li, Y. G. Investigation of Surface Tension and Interfacial Tension in Surfactant Solutions. *Ind. Eng. Chem. Res.* **2000**, *39*, 320.

(49) Chou, T.-J.; Tanioka, A.; Tseng, H.-C. Salting Effect on the Liquid-Liquid Equilibria for the Partially Miscible Systems of *n*-Propanol-Water and *i*-Propanol-Water. *Ind. Eng. Chem. Res.* **1998**, *37*, 2039.

(50) Economou, I. G.; Tsionopoulos, C. Associating models and mixing rules in equation of state for water/hydrocarbon mixtures. *Chem. Eng. Sci.* **1997**, *52*, 511.

(51) Yakoumis, I. V.; Kontogeorgis, G. M.; Voutsas, E. C.; Hendriks, E. M.; Tassios, D. P. Prediction of phase equilibria in binary aqueous systems containing alkanes, cycloalkanes, and alkenes with the cubic-plus-association equation of state. *Ind. Eng. Chem. Res.* **1998**, *37*, 4175.

(52) Voutsas, E. C.; Boulougouris, G. C.; Economou, I. G.; Tassios, D. P. Water-hydrocarbon phase equilibria using the thermodynamic perturbation theory. *Ind. Eng. Chem. Res.* **2000**, *39*, 797.

(53) O'Sullivan, T. D.; Smith, N. O. Solubility and partial molar volume of nitrogen and methane in water and in aqueous sodium chloride from 50 to 125 °C and 100 to 600 atm. *J. Phys. Chem.* **1970**, *74*, 1460.

(54) Price, L. C.; Blount, W. C.; McGowan, D.; Wenger, L. *Proc. Conf. Geopressured-Geothermal Energy*; Bebout, D. G., Bachman, A. L., Eds.; Louisiana State University: Baton Rouge, LA, 1982.

(55) Nezbeda, I.; Kolafa, J.; Kalyuzhnyi, V. Primitive model of water. II. Theoretical results for the structure and thermodynamic properties. *Mol. Phys.* **1989**, *68*, 143.

(56) Nezbeda, I.; Iglesias-Silva, G. A. Primitive model of water. III. Analytic theoretical results with anomalies for the thermodynamic properties. *Mol. Phys.* **1990**, *69*, 767.

(57) Galindo, A.; Whitehead, P. J.; Jackson, G.; Burgess, A. N. Predicting the High-Pressure Phase Equilibria of Water + *n*-

Alkanes Using a Simplified SAFT Theory with Transferable Intermolecular Interaction Parameters. *J. Phys. Chem.* **1996**, *100*, 6781.

(58) Galindo, A.; Whitehead, P. J.; Jackson, G.; Burgess, A. N. Predicting the Phase Equilibria of Mixtures of Hydrogen Fluoride with Water, Difluoromethane (HFC-32), and 1,1,1,2-Tetrafluoroethane (HFC-134a) Using a Simplified SAFT Approach. *J. Phys. Chem. B* **1997**, *101*, 2082.

(59) Garcia-Lisbona, M. N.; Galindo, A.; Jackson, G.; Burgess, A. N. Predicting the high-pressure phase equilibria of binary aqueous solutions of 1-butanol, *n*-butoxyethanol and *n*-decylpentaoxyethylene ether (C₁₀E₅) using the SAFT-HS approach. *Mol. Phys.* **1998**, *93*, 57.

(60) Garcia-Lisbona, M. N.; Galindo, A.; Jackson, G.; Burgess, A. N. An examination of the cloud curves of liquid-liquid immiscibility of aqueous solutions of alkyl-polyoxyethylene surfactants using the SAFT-HS approach with transferable parameters. *J. Am. Chem. Soc.* **1998**, *120*, 4191.

(61) Economou, I. G.; Donohue, M. D. Chemical, Quasi-Chemical and Perturbation Theories for Associating Fluids. *AIChE J.* **1991**, *37*, 1875.

(62) Suresh, S. J.; Elliott, J. R. Multiphase Equilibrium Analysis via a Generalized Equation of State for Associating Mixtures. *Ind. Eng. Chem. Res.* **1992**, *31*, 2783.

(63) Jackson, G.; Gubbins, K. E. Mixtures of associating spherical and chain molecules. *Pure Appl. Chem.* **1989**, *61*, 1021.

(64) McCabe, C.; Jackson, G. SAFT-VR Modelling of the Phase Equilibrium of long-chain *n*-alkanes. *Phys. Chem. Chem. Phys.* **1999**, *1*, 2057.

(65) McCabe, C.; Galindo, A.; Garcia-Lisbona, M. N.; Jackson, G. Examining the Adsorption (Vapor-Liquid Equilibria) of Short-Chain Hydrocarbons in Low-Density Polyethylene with the SAFT-VR Approach. *Ind. Eng. Chem. Res.* **2001**, *40*, 3835.

(66) Wagner, W.; Kruse, A. *Properties of water and steam*; Springer: Germany, 1998.

(67) Weast, R. C.; Astle, M. J. *Handbook of Chemistry and Physics*; CRC Press: Boca Raton, FL, 1981.

(68) Rowlinson, J. S.; Swinton, F. L. *Liquids and liquid mixtures*; Butterworth Scientific: London, UK, 1982.

(69) Boublik, T. Hard-Sphere Equation of State. *J. Chem. Phys.* **1970**, *53*, 471.

(70) Mansoori, G. A.; Carnahan, N. F.; Starling, K. E.; Leland, T. W. Equilibrium Thermodynamic Properties of the Mixture of Hard Spheres. *J. Chem. Phys.* **1971**, *54*, 1523.

(71) Barker, A.; Henderson, D. What is "liquid"? Understanding the states of matter. *Rev. Mod. Phys.* **1975**, *48*, 587.

(72) Wertheim, M. S. Fluids with Highly Directional Attractive Forces. I. Statistical Thermodynamics. *J. Stat. Phys.* **1984**, *35*, 19.

(73) Wertheim, M. S. Fluids with Highly Directional Attractive Forces. II. Thermodynamic Perturbation Theory and Integral Equations. *J. Stat. Phys.* **1984**, *35*, 35.

(74) Wertheim, M. S. Fluids with Highly Directional Attractive Forces. III. Multiple Attraction Sites. *J. Stat. Phys.* **1986**, *42*, 459.

(75) Wertheim, M. S. Fluids with Highly Directional Attractive Forces. IV. Equilibrium Polymerization. *J. Stat. Phys.* **1986**, *42*, 477.

(76) Jackson, G.; Chapman, W. G.; Gubbins, K. E. Phase equilibria of associating fluids. Spherical molecules with multiple bonding sites. *Mol. Phys.* **1988**, *65*, 1.

(77) Chapman, W. G.; Jackson, G.; Gubbins, K. E. Phase equilibria of associating fluids. Chain molecules with multiple bonding sites. *Mol. Phys.* **1988**, *65*, 1057.

(78) Chapman, W. G. Prediction of the Thermodynamic Properties of Associating Lennard-Jones Fluids: Theory and simulation. *J. Chem. Phys.* **1990**, *93*, 4299.

(79) Waisman, E.; Lebowitz, J. L. Exact Solution of an Integral Equation for the Structure of a Primitive Model of Electrolyte. *J. Chem. Phys.* **1970**, *52*, 4307.

(80) Press, W. H.; Teukolsky, S. A.; Vetterling, W. T.; Flannery, B. P. *Numerical Recipes in Fortran*; Cambridge University Press: Cambridge, 1986.

(81) Scott, R. L.; van Konynenburg, P. H. Critical Lines and Phase Equilibria in Binary Van der Waals Mixtures. *Discuss. Faraday Soc.* **1970**, *49*, 87.

(82) van Konynenburg, P. H.; Scott, R. L. Critical Lines and Phase Equilibria in Binary Van der Waals Mixtures. *Philos. Trans. R. Soc. A* **1980**, *298*, 495.

(83) Errington, J. R.; Boulougouris, G. C.; Economou, I. G.; Panagiotopoulos, A. Z.; Theodorou, D. N. Molecular simulation of

phase equilibria for water + methane and water + ethane mixtures. *J. Phys. Chem. B* **1998**, 102, 8865.

(84) Smit, B.; Karaborni, S.; Siepmann, J. I. Computer simulations of vapour-liquid phase equilibria of *n*-alkanes. *J. Chem. Phys.* **1995**, 102, 2126.

(85) Martin, M. G.; Siepmann, J. I. Transferable potentials for phase equilibria I: united atom description of *n*-alkanes. *J. Phys. Chem. B* **1998**, 102, 2569.

(86) Danneil, A.; Todheide, K.; Frank, E. U. Verdampfungsgleichgewichte und kritische Kurven in den Systemen Äthan/Wasser und *n*-Butan/Wasser bei hohen Drücken. *Chem. Ing. Technol.* **1967**, 39, 816.

(87) de Loos, T. W.; Wijen, A. J. M.; Diepen, G. M. Phase equilibria and critical phenomena in fluid (propane + water) at high pressures and temperatures. *J. Chem. Thermodyn.* **1980**, 12, 193.

(88) de Loos, T. W.; Penders, G.; Lichtentaler, R. N. Phase equilibria and critical phenomena in fluid (*n*-hexane + water) at high pressures and temperatures. *J. Chem. Thermodyn.* **1982**, 14, 84.

(89) de Loos, T. W.; van Drop, J. H.; Lichtentaler, R. N. Phase

Equilibria and Critical Phenomena in Fluid (*n*-alkane + water) Systems at High Pressures and Temperatures. *Fluid Phase Equilib.* **1983**, 10, 279.

(90) Smith, B. D.; Srivastava, R. *Thermodynamic data for pure compounds*; Elsevier: Amsterdam, The Netherlands, 1986.

(91) Fletcher, D. A.; McMeeking, R. F.; Parkin, D. The United Kingdom Chemical Database Service. *J. Chem. Inf. Comput. Sci.* **1996**, 36, 746.

(92) Li, Y. K.; Ngheim, L. X. Phase Equilibria of Oil, Gas and Water/Brine Mixtures from a Cubic Equation of State and Henry's Law. *Can. J. Chem. Eng.* **1986**, 64, 486.

(93) Tsonopoulos, C.; Wilson, G. M. High Temperature Mutual Solubilities of Hydrocarbons and Water, Part I: Benzene, Cyclohexane and *n*-Hexane. *AIChE J.* **1983**, 29, 990.

Received for review November 14, 2002

Revised manuscript received May 20, 2003

Accepted May 21, 2003

IE020918U